Biomolecular Detection and Quantification 10 (2016) 15–23

Contents lists available at ScienceDirect

Biomolecular Detection and Quantification

journal homepage: www.elsevier.com/locate/bdq

Review Article

# Fundamentals of multiplexing with digital PCR

Alexandra S. Whale[a,*], Jim F. Huggett[a], Svilen Tzonev[b]

[a] Molecular and Cell Biology Team, LGC, Queens Road, Teddington, Middlesex TW11 0LY, United Kingdom
[b] Digital Biology Centre, Bio-Rad Laboratories Inc., 5731 West Las Positas Boulevard, Pleasanton, CA 94588, United States

ARTICLE INFO

*Article history:*
Received 28 March 2016
Received in revised form 13 May 2016
Accepted 17 May 2016
Available online 27 May 2016

*Keywords:*
dPCR
Digital PCR
Duplex
Higher order multiplexing
Multiplexing

ABSTRACT

Over the past decade numerous publications have demonstrated how digital PCR (dPCR) enables precise and sensitive quantification of nucleic acids in a wide range of applications in both healthcare and environmental analysis. This has occurred in parallel with the advances in partitioning fluidics that enable a reaction to be subdivided into an increasing number of partitions. As the majority of dPCR systems are based on detection in two discrete optical channels, most research to date has focused on quantification of one or two targets within a single reaction. Here we describe 'higher order multiplexing' that is the unique ability of dPCR to precisely measure more than two targets in the same reaction. Using examples, we describe the different types of duplex and multiplex reactions that can be achieved. We also describe essential experimental considerations to ensure accurate quantification of multiple targets.

© 2016 The Author(s). Published by Elsevier GmbH. This is an open access article under the CC BY-NC-ND license (http://creativecommons.org/licenses/by-nc-nd/4.0/).

**Contents**



* Corresponding author.
*E-mail address:* alexandra.whale@lgcgroup.com (A.S. Whale).

http://dx.doi.org/10.1016/j.bdq.2016.05.002
2214-7535/© 2016 The Author(s). Published by Elsevier GmbH. This is an open access article under the CC BY-NC-ND license (http://creativecommons.org/licenses/by-nc-nd/4.0/).

## 1. Introduction

Digital PCR (dPCR) involves the partitioning of a PCR reaction into a number of smaller partitions so that a proportion of them contain no template molecules [1,2]. PCR is then performed to determine the proportion of positive (with amplification) and negative (no amplification) partitions. This subdivision enables quantification to be performed using established statistical models that are independent of a calibration curve [3] and increases the precision of the quantification [4–8]. There are two broad mechanisms for the subdivision of a reaction: partitioning using nanofluidics to load the reaction into prefabricated chambers, or by generation of water-in-oil emulsions. The partition volume can vary from 4.4 μL down to 5 pL and the partition number in a reaction can vary from 496 up to 10 million partitions depending on the dPCR platform used [9].

dPCR has been used in a wide range of research areas that include measurement of copy number variation in genetically modified organisms [10,11] and for karyotyping plants [12,13] as well as in human disease models such as gene expression [14] and epigenetic control of gene expression in cancer [8,15,16], gene amplification in cancer [6,17] and prenatal fetal karyotyping [18]. The other major application for dPCR is in the detection of rare sequence variants, which in standard qPCR can be lost within the high abundant background type [17,19]. Such measurements have been evaluated in many human diagnostic areas that include cancer stratification [20,21], antimicrobial resistance monitoring [22,23], prenatal diagnostics [24,25] and monitoring of transplant organ rejection [26]. Most recently, dPCR is finding multiple applications in the emerging field of liquid biopsy, where solid tumors are profiled non-invasively based on detection of tumor-related nucleic acids in blood or other anatomical liquids [27–29].

### 1.1. Detection of amplification

dPCR relies on the ability to distinguish between partitions that contain amplicons and those that do not. Partitions that contain amplicons can be identified by the presence of increased fluorescence using a variety of detection chemistries common to qPCR such as intercalating DNA dyes or fluorophore-labelled oligonucleotides [30]. Following PCR cycling, the fluorescence end-point signal associated with each partition is measured by the reader instrument. This signal can be plotted on a one-dimensional (1D) scatter graph, with the event (partition) number along the x-axis and the fluorescent amplitude along the y-axis. In a well optimized assay, two visually distinct populations are observed; positive partitions that have high fluorescence, and negative partitions that have low (or background) fluorescence. An automatic threshold is set by the software to separate these two populations, however, for all the dPCR platforms it is possible for the user to manually set the threshold in the analysis software and this is described in more detail in Section 4.4.

### 1.2. Basics of quantification

Experimentally, we can only distinguish between negative partitions (containing zero targets) and positive partitions (containing one or more targets). The fundamental assumption of independent distribution of target molecules into equal volume partitions means that the number of targets per partition will follow a standard Poisson distribution. The Poisson model is defined by a single parameter 'λ'—the average number of targets per partition. Historically, λ is represented as:

$$\lambda = -\ln\left(1 - \frac{k}{n}\right) \quad (1)$$

where $n$ is the total number of partitions detected and $k$ is the number of positive partitions detected as defined in the "Minimum Information for Publication of Quantitative Digital PCR Experiments" (dMIQE) guidelines (3). Eq. (1) is written in this way to use the positive partitions (k) as a proportion of total partitions (n). These were chosen as working with positive partitions is more intuitive to the user. However, λ is really calculated using the negative partitions as the proportion of positive partitions in Eq. (1), $k/n$ is subtracted from 1.

The negative partitions are arguably more informative than the positive partitions since we know each negative partition contains zero copies of the target, while a positive partition may contain one or more copies of the target. When multiplexing, λ needs to be calculated for each targets individually and the notion of a positive partition becomes dependent on the target of interest. In a sense a 'positive' partition becomes even less informative as it may contain 1 or more copies of multiple targets. If $w$ denotes the number of partitions that are negative for a target and so $n = k + w$. By substituting $w$ into Eq. (1) we can calculate λ in terms of the number of negative partitions, $\lambda = -\ln(w/n)$, that can then be rearranged to give Eq. (2):

$$\lambda = \ln(n) - \ln(w) \quad (2)$$

This arrangement allows for easier generalization in the case of multiple targets. The full advantage of Eq. (2) is realised when we want to quantify a target in a sample without using all the partitions in that reaction. Specific scenarios and examples where this is useful are given below in the relevant sections along with the appropriate generalization of Eq. (2).

For any given experiment, both Eqs. (1) and (2) provide an estimate of λ and the uncertainty of λ can be calculated using equations that are described elsewhere [6,31]. In certain cases the assumption of independent target distribution may not hold, for example, with close tandem copies [6] or denatured DNA [32,33]. Furthermore, molecular dropout may occur, where a molecule fails to amplify and so a partition that initially contained a molecule is wrongly classified as negative [34]. In such cases the estimate of λ will not be accurate as the binomial distribution is no longer appropriate.

## 2. Duplex assays

Duplex assays enable concurrent amplification of two targets within a single reaction. This reduces technical errors, such as accumulated pipetting inaccuracy, thereby making it possible to measure smaller differences than the same comparison using parallel uniplex reactions [34]. Duplexing also reduces reagent and time needs. Duplex assays can be performed with intercalating DNA dyes or fluorophore-labelled oligonucleotides; the examples illustrated in this study use hydrolysis probes, but the theory holds true for other fluorophore-labelling strategies such as Scorpion or Amplifluor™ primer-probes or hybridisation probes such as Molecular Beacons [30].

In duplex hydrolysis probe assays, the two probes are typically labelled with a different dye to match the two detection channels. There are four possible configurations in terms of the number of primer pairs used in the reaction (1 or 2) and if the two probes bind the same region of the generated amplicon(s) (Table 1). Only three configurations are meaningful, since the fourth one is unlikely to occur where different primers generate amplicons containing the same probe binding site.

An alternative strategy for duplex reactions is to use a single-colour intercalating DNA dye, such as EvaGreen, to amplify amplicons of different sizes for the different targets; the targets are discriminated by the differences in the fluorescence ampli-

**Table 1**
Possible reaction configurations for duplex reactions.

| | | Number of primer pairs | |
|---|---|---|---|
| | | 1 | 2 |
| Probes binding | same region | Competing duplex reaction; e.g. rare mutant detection (Fig. 1B) | N/A |
| | different region | Non-competing (hybrid) duplex reaction (Fig. 1C) | Non-competing duplex reaction; e.g. copy number variation (Fig. 1A) |

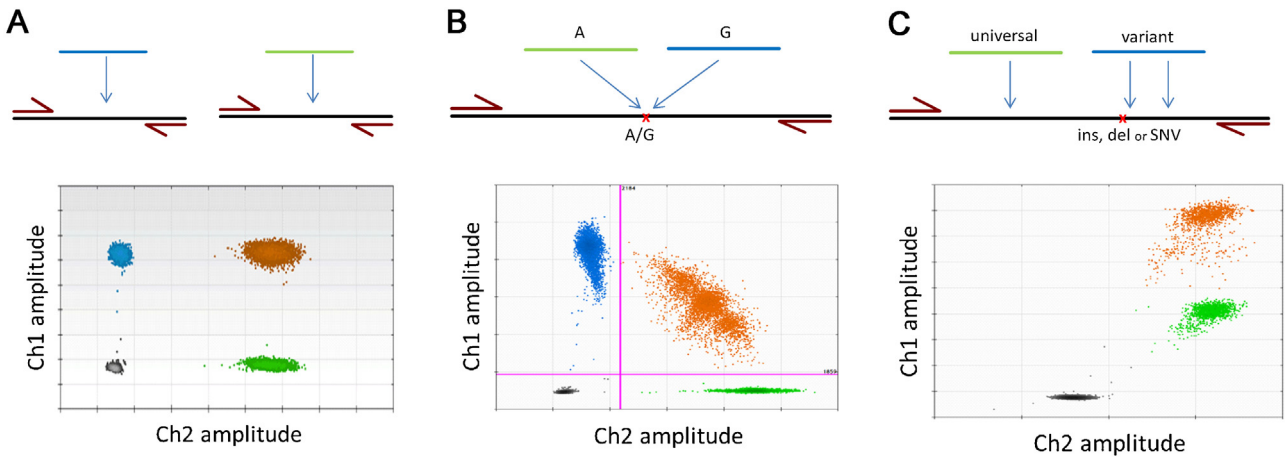


**Fig. 1.** Graphical outputs for duplexing strategies. All illustrative examples given here used the QX200™ Droplet Digital™ PCR System (Bio-Rad). A schematic is given for the primer and probe hybridisation arrangements with an example of the configuration of clusters in the 2D plot underneath. For each plot, the amplitude in channel 1 (ch1) is represented on the y-axis with the amplitude in channel 2 (ch2) represented on the x-axis. Four clusters are identified as single-positive for Ch1 (blue) and Ch2 (green), double-positive (orange) and double-negative (grey). (A) For non-competing duplex reactions, a rectangular conformation is observed between the four clusters. The amplitude of the double-positive cluster is approximately equal to that of the two single-positive clusters. (B) For competing duplex reactions, the four clusters have been pulled out of the rectangular conformation observed in (A). The double-positive cluster has dropped inwards and formed an arc across the scatter plot. (C) For non-competing (hybrid) duplex reactions, only three clusters are visible. Discrimination of the variant and double-positive clusters is not possible (all partitions are coloured orange).

tude associated with amplicon size [35]. This is often referred to as 'amplicon-size multiplexing'.

### 2.1. Non-competing duplex reactions (two primer pairs)

A standard duplex reaction generates two amplicons from two primer sets with the signal generated from a probe specific for each amplicon. Fig. 1A illustrates two targets, A and B, that are being quantified. A two-dimensional (2D) scatter graph can be generated, where the fluorescent amplitude of one probe channel (ch1), that represents target A, is plotted on the y-axis and the other probe channel (ch2), that represents target B, is plotted on the x-axis. In this graph a partition can fall into one of four possible clusters: (i) negative partitions that contain no amplified targets, positive partitions for (ii) target A or (iii) target B (collectively referred to as single-positive partitions), and (iv) positive partitions that contain a positive signal for both targets (double-positive partitions).

Typically, the four clusters are arranged in a rectangular configuration with the double-positive cluster having approximately the same amplitude in both channels as the single-positive clusters (Fig. 1A). In some cases the double-positive cluster may exhibit lower amplitude for one of the targets; this occurs when one amplicon is preferentially amplified at the expense of the other. Causes of this imbalance can include primer characteristics such as differences in melting temperature, secondary structure, or the primers negatively interfering with each other [36].

As long as thresholds can be set to separate the positive and negative partitions in each of the two probe channels then the estimation of the concentration of both targets using either Eqs. (1) or (2) will still be suitable. The typical result produced with such assay configurations is the *ratio* of the concentrations of the two targets. Examples of this type of reaction have been used in the identification of *HER2* amplification in breast cancer patients [37–39].

### 2.2. Competing duplex reactions (one primer pair with two probes binding the same region)

An alternative duplex format amplifies two amplicons using a single pair of primers. The identity of the two amplicons is specified by the signal from the bound probe; one probe for each amplicon. This is a typical configuration for quantification of localised variants that include single nucleotide polymorphisms (SNP), single nucleotide variants (SNV) and small insertions or deletions. The specificity of the variant detection is conferred by one of the two probes; one for the abundant or wild type (WT) sequence and one for the variant. Examples of this type of reaction have been used in the identification of the EGFR mutations in cell free DNA extracted from plasma in lung cancer patients [27,40] and BRAF mutations in melanoma [41,42].

Similar to the non-competing duplex reaction, four clusters of partitions are generated. However, unlike non-competing duplex reactions, the double-positive cluster forms an arc conformation that spans the two single-positive clusters (Fig. 1B). This is primarily caused by a phenomenon caused partition specific competition (PSC) described in more detail in Section 4.3. Quantification can be harder as the competitive nature of the reaction in the double-positive partitions can make it difficult to position the thresholds for each probe channel. However, once thresholds are set to separate the four clusters, quantification of each target can be performed as described above. The typical result produced with such assay configurations is the *fractional abundance* of the variant target relative to the sum of abundant and variant targets. Alternative

reporting metrics are the number of variant copies per volume of the sample, e.g. copies/mL of plasma.

### 2.3. Non-competing (hybrid) duplex reactions

The third configuration of duplex reactions using probes includes the amplification of a single amplicon with two non-competing probes; these are often referred to as "Wild-Type-negative" or "drop-off" assays. The universal (or reference) probe targets an area of the amplicon that is not expected to be variable and thus, provides a reference for the *total* number of molecules present in the sample irrespective of sequence. The variant probe targets the area of the amplicon that is expected to contain one or more variants. A typical use for this type of assay is in detection of a broader set of possible mutations than can be covered by a single probe, for example, exon 19 deletions in the EGFR gene [27].

In this configuration, there are only three visible clusters (Fig. 1C): (i) negative partitions that contain no targets for either probe, (ii) single-positive partitions for the universal probe (WT only partitions) and (iii) positive partitions that contain a signal from both variant and universal probes (combined cluster). The missing single-positive cluster (variant only partitions) is subsumed into the combined cluster since the universal probe always produces a signal in the presence of any amplicon. For quantification of the targets we will use Eq. (2) and define $c_0$ as the number of partitions in the double-negative cluster, $c_{wt}$ for the WT only cluster and $c_{combined}$ for the combined cluster:

$$\lambda_{variant} = \ln(c_0 + c_{wt} + c_{combined}) - \ln(c_0 + c_{wt}) \quad (3)$$

$$\lambda_{wt} = \ln(c_0 + c_{wt}) - \ln(c_0) \quad (4)$$

Here we have extended Eq. (2) to use the relevant number of partitions for the different targets. Eq. (3) uses all partitions, while Eq. (4) uses a subset of all partitions. These equations also assume there are no interactions between the targets so that the a priori binomial distributions of positive and negative partitions for each target are independent of each other. Since, the overall *precision* of dPCR measurements depends on the number of partitions used [43,44], the precision of $\lambda_{wt}$ is lower than the precision of $\lambda_{variant}$. However, the quantification *trueness* of both targets is the same in that they are both unbiased.

### 2.4. Duplexing using non-specific double stranded DNA binding dyes

Multiple targets can be quantified using a single double stranded DNA binding fluorescence dye, such as EvaGreen. This method exploits the relationship between the proportionate level of end-point fluorescence and amplicon size. An alternative strategy involves varying the primer concentration for the two different assays, whilst keeping the amplicons at comparable lengths. These types of reaction can be used to calculate the *ratio* of the concentrations between the two targets. Examples of this type of reaction have been used in the quantification of RPP30 and ACTB (amplicon multiplexing) and CNV identification of *MRGPRX1* in HapMap samples (primer multiplexing) [35] and the V600E point mutation in the *BRAF* gene [45]. When all canonical clusters of partitions can be resolved, quantification is done the standard way. In some cases, like in non-competing hybrid probe assays, one of the single positive clusters may be subsumed into the double positives. We can then apply the same strategy for full target quantification.

## 3. Higher order multiplexing

In traditional qPCR multiplexing reactions, targets are differentiated using one probe per target conjugated with dyes of different emission spectra. This approach restricts multiplexing to systems that can cope with multiple emission spectra to capture the fluorescence from the different probe dyes. There are currently two commercial systems, the Fluidigm BioMark™ and EP1™ systems and the recently commercialised Stilla Narcia™ System, that have the capacity to multiplex in four and three optical channels, respectively. The other commercially available dPCR systems are restricted to detection in two discrete optical channels. Despite this, it is possible to precisely measure more than two targets in the same reaction [46]. This is termed 'higher order multiplexing' and is a unique property of dPCR.

The fundamental idea behind higher order multiplexing is that the end-point fluorescence amplitude in each partition is a function of probe-dye conjugation and mixing, probe and primer concentrations and the type of targets that are present prior to amplification. Each partition is still detected individually and will be represented as an event in a 2D scatter plot. By understanding and deconvoluting the resulting patterns, multiple targets can be quantified simultaneously. When each partition can be unambiguously assigned to a cluster, the full statistical power can be used to achieve maximal precision and accuracy.

In some cases different clusters may overlap in 2D space and, as we observed with the non-competing duplex reactions (Section 2.3), it is still possible to quantify specifically, albeit at the expense of reduced precision. We will first cover the cases with full cluster discrimination (amplitude- or ratio-based multiplexing) and then describe the use of multiplex reactions that quantify the targets using only a subset of all partitions.

### 3.1. Amplitude-based multiplexing

In an amplitude-based multiplex assay, targets are detected with probes conjugated with a single dye but at a different final concentration in the end-point reaction. This approach is similar to the non-specific double stranded DNA binding dye approach (Section 2.4). This strategy can be modified to measure three or more targets per reaction. In our illustrated example, four targets are being quantified in a 'tetraplex' reaction (Fig. 2A). Targets A and B have relative concentrations of 50% and 100% of Ch2-labelled probes, respectively; while C and D have relative concentrations of 50% and 100% of Ch1-labelled probes, respectively, giving 16 ($2^4$) possible clusters in the 2D amplitude space.

For this set up, single, double, triple and quadruple-positive clusters arise as a partition can contain any combination of the target types. For most precise quantification, all 16 clusters need to be uniquely identified and the number of partitions in each cluster to be reliably counted (Fig. 2A). Defining the threshold positions for this set up is more complicated than those for duplex reactions. In the example shown, all 16 clusters can be identified and so estimate the concentration of each target can be achieved using either Eqs. (1) or (2). For example, the lasso tool can be used to select all the clusters that do not contain target B ($w_B$) (Fig. 2B) and using Eq. (2), the concentration of target B can be computed:

$$\lambda = \ln(n) - \ln(w_B) \quad (5)$$

A typical application for such multiplex assays could be for more accurate estimation of the *copy number* of a target such as the evaluation of DNA integrity extracted from paraffin embedded tissue [47].

### 3.2. Ratio-based multiplexing with complete cluster identification

In ratio-based multiplexing assays some targets are detected in the conventional way, while others are detected using two probes conjugated with different dyes. In the illustrated example three

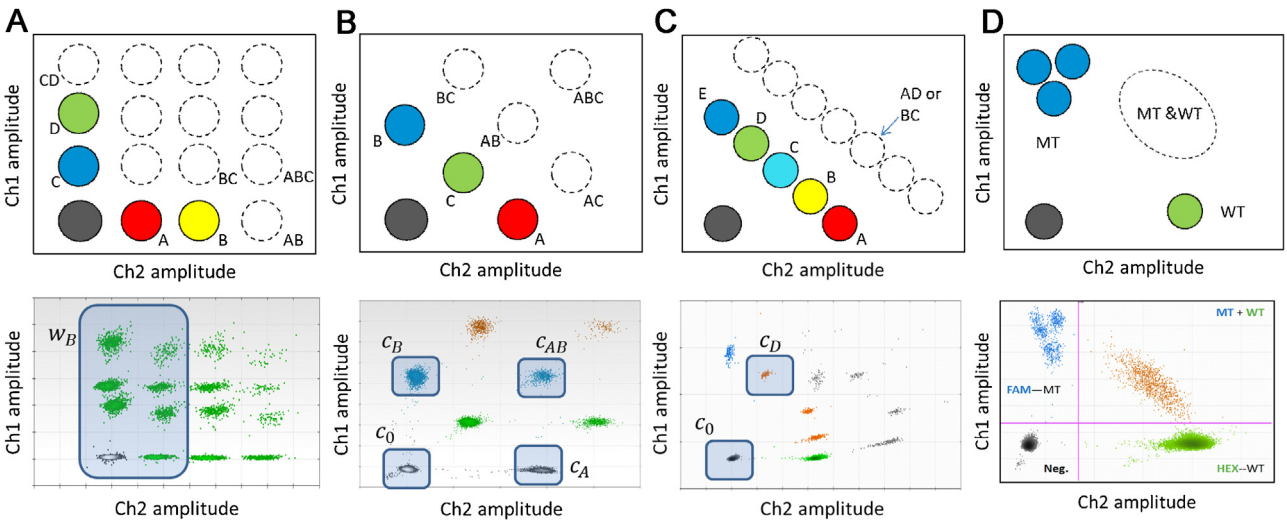


**Fig. 2.** Graphical outputs for higher order multiplexing strategies. All illustrative examples given here used the QX200™ Droplet Digital™ PCR System (Bio-Rad). For each multiplexing strategy a schematic and worked example of the configuration of clusters in the 2D plot is given with the amplitude in channel 1 (ch1) is represented on the y-axis with the amplitude in channel 2 (ch2) is represented on the x-axis. For each schematic the approximate location of the single target positive clusters are identified as solid coloured circles with the double or triple target positive clusters are shown as dotted circles. For the worked examples, the clusters are not pseudocoloured according to the target due to the limitations of the software. (A) For amplitude-based multiplexing, four independent targets are being quantified: targets A (100% Ch2-labelled probe), B (100% Ch2), C (50% Ch1) and D (100% Ch1) giving 16 possible clusters in the 2D amplitude space. For the worked example, all the clusters containing partitions that do *not* contain target B are lassoed ($w_B$). (B) For ratio-based multiplexing, three independent targets are being quantified: targets A (100% Ch2), B (100% Ch1) and C (50% Ch2 and 50% Ch1) giving 8 possible clusters in the 2D amplitude space. For the worked example, the four clusters used in the quantification are lassoed and labelled: negative cluster for all targets ($c_0$), single-positive for target B ($c_B$), single-positive for target A ($c_A$), and double-positive for targets A and B ($c_{AB}$). (C) For ratio-based non-discriminating multiplexing, five targets are being quantified: targets A (100% Ch2), B (75% Ch2/25%Ch1), C (50% Ch2/50% Ch1), D (25% Ch2/75% Ch1) and E (100% Ch1). A total of 32 combinations of clusters are possible, however, due to the ratios of the probes for the different targets, most are not uniquely identifiable. For example, a cluster containing both targets A and D (125% Ch2/75% Ch1) would not be distinguishable from a cluster containing both targets B and C (also 125% Ch2/75% Ch1). Therefore only the single-positive clusters can be used in the quantification. For the worked example, the two clusters used for the quantification of target D are lassoed: negative cluster for all targets ($c_0$) and single-positive cluster for target D ($c_D$). (D) For non-discriminating multiplexing the example of the *KRAS* mutations in codons 12 and 13 is shown. The 7 probes for the mutant SNVs are all conjugated with the Ch1-labelled probe and the WT probe is conjugated with the Ch2-labelled probe. Three diffuse clusters are visible in the mutant probe channel with a single cluster in the WT channel. The double-positive cluster is also visible. It is not possible to discriminate between the 3 mutant clusters and so this set up allows quantification of the total number of mutant sequences only.

targets are being quantified (Fig. 2B). Targets A and B have relative concentrations of 100% Ch2- and 100% Ch1-labelled probes, respectively. Target C has relative concentrations of 50% Ch2- and 50% Ch1-labelled probes. The expected location of the target C single-positive cluster is in between those of targets A and B, where both probe channels have a 50% reduction in fluorescent amplitude. Including the double- and triple-positive clusters gives a total of 8 ($2^3$) identifiable clusters for all possible combinations of the three targets.

In this example, we can use either Eqs. (1) or (2) to quantify the number of target molecules as described in the previous section. However, the full advantage of using Eq. (2) over Eq. (1) can be illustrated when we want to quantify based on a subset of clusters. For example, we might want to exclude all clusters that contain target C from the quantification and so use only the clusters that *do not* contain target C (Fig. 2B). Therefore, the total number of the partitions in the reaction and the number of partitions that are negative for target B are defined as:

$$n_{notC} = c_0 + c_A + c_B + c_{AB} \quad (6)$$

$$w_B = c_0 + c_A \quad (7)$$

From this we can then use Eq. (2) to estimate the concentration of target B:

$$\lambda_B = \ln(c_0 + c_A + c_B + c_{AB}) - \ln(c_0 + c_A) \quad (8)$$

Whether we use all partitions or a subset of partitions, we will achieve unbiased estimates, as long as there is no linkage between the targets (see Section 4.1). We may need to use fewer clusters if some clusters are not uniquely identifiable, poorly defined or not all accounted for in the reaction (a sample may not contain target C). Again, this method enables us to preserve the accuracy while giving some ground on precision.

### 3.3. Ratio-based multiplexing with incomplete cluster identification

In some cases, a careful selection of the ratios of the probes would allow an operator to multiplex even more targets in a single reaction. This may require use of an incomplete set of clusters. In the illustrated example five targets are quantified (Fig. 2C). Targets A and E have relative concentrations of 100% Ch2 and Ch1-labelled probes, respectively. Targets B, C and D have labelled Ch1 and Ch2-labelled probes at varying ratios. In this setup we should see a total of 32 ($2^5$) different combinations of the five targets; however, many of these clusters may not be uniquely identifiable. For example, the position of the double-positive partitions containing targets A and D may overlap with that of the double-partitions containing targets B and C (Fig. 2C). In many cases higher order positives also cannot be uniquely identified. Nevertheless, one can achieve accurate quantification by using only the single-positive clusters. For example, to calculate the concentration of target D using Eq. (2) we only need to count the number of partitions in the negative cluster ($c_0$) and the single-positive cluster that contains target D ($c_D$) (Fig. 2C):

$$\lambda_D = \ln(c_0 + c_D) - \ln(c_0) \quad (9)$$

This method allows for interrogation of multiple targets at the expense of reduced precision. As before the estimates for average occupancies for each target are unbiased.

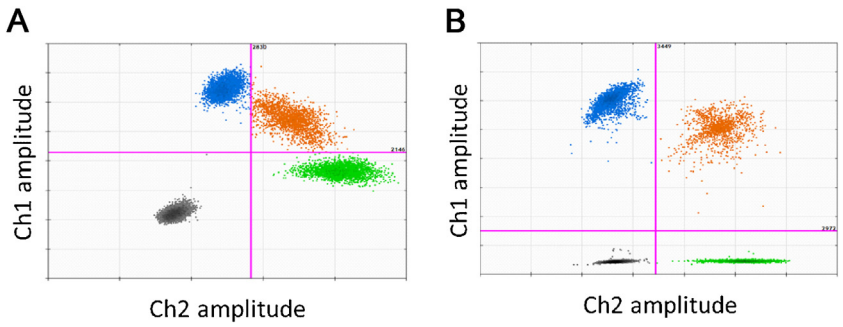


**Fig. 3.** Considerations for accurate quantification. All illustrative examples given here used the QX200™ Droplet Digital™ PCR System (Bio-Rad) using duplex reactions; however, all of these are relevant for higher order multiplexing strategies. (A) For the analysis of a probe-competing duplex reactions to quantify a transition mutation. Cross-hybridisation of the probes caused by either mismatched binding of the probes or filter bleed-though can be visualised as a 'leaning' (blue) or 'lifting' (green) of the single-positive clusters. This can impact on positioning the thresholds to separate the four clusters. (B) Analysis of a probe-competing duplex reaction to detect a 3 amino acid deletion mutation to illustrate that mismatched binding of the probes does not cause the 'leaning' or 'lifting' of the clusters compared with that observed in (A).

### 3.4. Non-discriminating multiplexing

To complete our survey of multiplexing assays we next describe the case where some targets are detected but will never be uniquely identified as this is not required by the application. In such experiments, we wish to report the presence and quantity of any combination of the targets of interest. A typical example is presented in Fig. 2D where all 7 mutations in the *KRAS* gene, exons 12 and 13, are Ch1-labelled probes, while WT has a Ch2-labelled probe. The 7 mutant species generate 3 diffuse mutant clusters but we combine the counts of those for the purposes of quantification.

Identification of the specific mutation is not required as the fundamental question is 'does this sample contain mutations' and so the reaction performs a screening role. Such screening assays are useful when the expected prevalence of mutations is low and it is more efficient to only determine the specific mutation in the sample once the presence of a mutation has been confirmed. Multiplex screening in this style typically leads to reduced sensitivity limits than when detecting individual targets. For quantification we can use Eq. (2) as described for competing duplex reactions (Section 2.2).

## 4. Considerations for accurate quantification

Several factors are important for accurate quantification of multiplexed assays. These include target linkage, probe specificity and competition, differential PCR efficiencies. Any factor that distorts the location and uniqueness of clusters needs to be taken into consideration, especially when multiple targets are measured. Due to the extra level of complexity in these types of reactions, care should be taken to recognise and reduce these effects by rigorous optimisation to ensure accurate estimation of λ. In this section we describe in more detail the causes of these factors and the effects they can have on the quantification if they are not recognised and accounted for.

### 4.1. Linked targets

Quantification of linked targets by dPCR may cause problems as the assumptions for random and independent (Poisson) distribution of target molecules may not hold. Tandem repeat copies of the same target would co-localize in the same partition more frequently than by chance, which will lead to an *underestimation* of the true number of copies. In the case of two different targets in *cis* and nearby, there will be an excess of double positive partitions. We can measure the concentration of each target using standard approaches but may miss the fact the targets are indeed linked [48]. Current standard analysis tools can report the concentration of the linked molecules using linkage-based assays to measure *cis* versus *trans* configuration of targets and potential structural rearrangements [49]. This can be further extended to determine the degree of DNA fragmentation under different extraction conditions. Care needs to be taken when using a reduced set of clusters for quantification as this approach is in general valid under the assumption of no linkage or higher order target correlations.

### 4.2. Specificity

The design of an assay for detection of SNVs is naturally somewhat constrained. In an ideal scenario, the two probes will have stringent enough specificity, such that only 'fully matched hybridisation' will occur; the WT probe will hybridise to the amplicons containing the WT sequence only and the variant probe will hybridise to the amplicons containing the mutant sequence only. However, for many SNV assays, cross-(mismatched) hybridisation of the probes does occur. As mismatches occur with lower efficiency than matches, this will lead to 'leaning' or 'lifting' of the single-positive partitions in the 2D scatter plot (Fig. 3A). For comparison, cross-hybridisation is less pronounced when the probe targets a variation involving two or more nucleotide deletions or insertions (Fig. 3B).

This loss of specificity can be further compounded by optical bleed-through, where the fluorescence from a dye is picked up by both detection channels (often referred to as 'filter cross-talk'). This effect produces a similar 'lifting' of the clusters and may be hard to separate from probe cross-hybridization effects. Filter cross talk can be alleviated by careful selection of conjugated dyes that match optical detection systems and by adjustment of signal processing parameters in the analysis software where this is possible.

### 4.3. Effects of partition specific competition (PSC)

In dPCR any partition is a miniature reaction by itself. As such, competition effects during PCR may be present. The degree to which those matter will depend on factors such as which targets and how many molecules of each target are present in each partition, differential amplification efficiencies, DNA accessibility and template quality. Every partition will follow standard amplification trajectory with an early exponential amplification followed by a saturation phase.

For CNV-like duplex assays (Section 2.1), there is no direct probe competition. However, in the double-positive partitions (where both targets are present at start) there will be two PCR reactions competing for resources. In the case where efficiencies are roughly balanced, the amplitudes of the double-positive partitions will be similar to the amplitudes of single-positive partitions. An imbal-

**Table 2**
Experimental setup to assess an assay in duplex (with WT or variant templates).

| Approximate template λ | | Reaction format | Purpose |
|---|---|---|---|
| Variant | WT/other | | |
| 0.7 | – | Duplex | Evaluate SNV specificity (probe cross-hybridisation & filter bleed-through) |
| – | 0.7 | Duplex | |
| 0.7 | – | Uniplex | Evaluate filter bleed-through |
| | 0.7 | Uniplex | |
| 0.7 | 0.7 | Duplex | Evaluate partition specific competition and specificity |
| <0.05 | – | Duplex | Evaluate SNV sensitivity and performance at low concentration (linearity) |
| <0.025 | <0.025 | Duplex | Evaluate probe cross-hybridisation & filter bleed-through |

ance of efficiencies may result in one amplicon outcompeting the other which will manifest as a 'drop' in amplitude in one probe channel relative to the canonical rectangular configuration.

In the case of SNV-like assays (Section 2.2), the competition is constrained to the probes only. A curious phenomenon occurs for some assays to give an arc-shaped cluster that exhibits a clear sub-cluster structure (Fig. 1B). The source of the sub-clusters in this case is the different initial conditions for double-positive partitions; some may start with one molecule of each WT and variant, while some may have ratios of the two molecules such as 2:1, 1:2, 3:1 and so on. When the assay has very specific probes for each target these different initial conditions will be still detectable in the final end-point picture.

### 4.4. Other factors that can effect quantification

While a dPCR reaction generates positive and negative partitions, in many cases, a subset of partitions will be detected that have a signal that is higher than the negative but lower than the positive partitions. These partitions are often referred to as 'rain'. There are a number of factors that affect the amount of rain observed and these include, but are not limited to template type (e.g. plasmid, genomic DNA or cDNA), template conformation (e.g. linear or supercoiled), template integrity (e.g. high molecular weight or fragmented), assay specificity, reduced PCR efficiency or the presence of inhibitors in the reaction [3,34,50,51].

In these situations, the user can either use the threshold position as set by the in-built software algorithms for the specific dPCR platforms, or they can manually set the threshold, the latter of which can be subjective. In order to reduce the subjective nature of the user setting and to try and standardise the data analysis method, three recent publications have described methods to aid operators to set the thresholds appropriately. One describes a JavaScript code 'definetherain' where the threshold is determined by the k-nearest neighbour algorithm of a control sample [52]. The second method uses a manual global threshold (MTg) approach that is based on the amplitude signal observed in negative control samples [53]. The third method describes a procedure based on kernel density estimation using the end-point fluorescent readings from each partition [54]. In general, well designed assays will provide enough 'white space' between the positives and negatives, so presence of 'rain' is a clear indication of sample-related problems. Whether to include the rain partitions into the positive or negative populations depends on the desired performance. In some cases, where many target copies are present, rain partitions make up a small fraction of the total partition number. In cases where detection of true rare variant molecules is critical, it may be advisable to bias thresholding to exclude the rain from the positive partition count (and therefore include the rain in the negative partitions). In most cases, careful analysis of known negative samples should be used to help guide decisions related to the rain. Only in very rare cases does it make sense to exclude rain completely from analysis; it should be classified as either the positive or negative partitions.

### 4.5. Suggested experimental setup to assess dPCR assays

In order to identify the effects from experimental factors that can influence the clustering of an assay, we have developed a suggested experimental set up to assist with assay optimisation (Table 2). By measuring performance on control samples at particular target occupancies in duplex and singleplex reactions and comparing the 2D scatter plots a researcher can identify specificity and PSC effects. Control samples containing either only WT or variant molecules can be evaluated in both duplex and uniplex reactions. The suggested concentration for these control samples is to achieve a λ of approximately 0.7 as at this concentration approximately half the partitions are positive and half are negative for each target.

In the 2D plot, filter bleed-through is identified in the *uniplex* reactions as a 'leaning' or 'lifting' of the corresponding single-positive cluster. In the absence (or minimal effect) of filter bleed-through, probe cross-hybridisation would be identified by the 'lifting' and 'leaning' of the single-positive clusters in the *duplex* reactions (Fig. 3A). A similar set up can be designed for higher order multiplexing experiments with controls for each target.

As it is the presence of both target molecules within a partition that causes the PSC, analysis with duplex reactions of a sample containing a 50:50 mix of the WT and mutant molecules, with an expected λ value of 0.7 for each molecule would give roughly equal numbers of partitions in each of the four clusters (Table 2 and Fig. 3B). Comparison of this 50:50 mix with WT-only and variant-only control samples should demonstrate a similar concentration of each molecule (Table 2).

Sample concentration can also impact on the PSC; as the sample concentration increases, the likelihood of multiple copies of each molecule being randomly distributed into each partition also increases. This will increase the cross-hybridisation and PSC effects in the single-positive and double-positive partitions, respectively. Diluting the sample so that there is a smaller proportion of partitions in the double-positive cluster may improve the quantification by reducing the PSC effects. For example, a dilution of each of the three samples described to generate concentrations with approximate λ values of <0.05 for the WT-only and variant-only samples and a λ value of <0.025 for the 50:50 mix (Table 2). This low concentration would ensure that almost all the positive partitions are located in the single-positive cluster.

## 5. Conclusions

The transition of digital PCR in the last decade from a niche technology into the mainstream holds significant potential to transform our ability to perform precise and highly accurate quantitative molecular analyses in a wide range of applications. In many cases we can now perform molecular counting experiments with multiple targets. This report has illustrated strategies and pitfalls in achieving such multiplexing. We showed how important it is to correctly classify the partitions and how rich the analysis space can be. While the industry is focussing on improving the workflow,

number of partitions and detection channels, dPCR will realize its full potential when the analysis of such rich cases is transformed into simple and intuitive end-user solutions. Furthermore, development of appropriate reference materials for assay optimisation for duplex and higher order multiplexing reactions that enable confident identification of the different partition clusters would be hugely beneficial.

## Competing interest

There are no competing interests for ASW and JFH. ST is an employee of Bio-Rad Laboratories who make and supply dPCR instruments and reagents.

## Acknowledgments

The work described in the manuscript was partially funded by the United Kingdom National Measurement System (NMS) and the European Metrology Research Programme (EMRP) joint research project (SIB54) Bio-SITrace (http://biositrace.lgcgroup.com) which is jointly funded by the EMRP participating countries within EURAMET and the European Union.

## References

[1] B. Vogelstein, K.W. Kinzler, Digital PCR, Proc. Natl. Acad. Sci. U. S. A. 96 (1999) 9236–9241.
[2] P.J. Sykes, S.H. Neoh, M.J. Brisco, E. Hughes, J. Condon, A.A. Morley, Quantitation of targets for PCR by use of limiting dilution, Biotechniques 13 (1992) 444–449.
[3] J.F. Huggett, C.A. Foy, V. Benes, K. Emslie, J.A. Garson, R. Haynes, J. Hellemans, M. Kubista, R.D. Mueller, T. Nolan, The digital MIQE guidelines: minimum information for publication of quantitative digital PCR experiments, Clin. Chem. 59 (2013) 892–902.
[4] S. Weaver, S. Dube, A. Mir, J. Qin, G. Sun, R. Ramakrishnan, R.C. Jones, K.J. Livak, Taking qPCR to a higher level: analysis of CNV reveals the power of high throughput qPCR to enhance quantitative resolution, Methods 50 (2010) 271–276.
[5] R. Sanders, J.F. Huggett, C.A. Bushell, S. Cowen, D.J. Scott, C.A. Foy, Evaluation of digital PCR for absolute DNA quantification, Anal. Chem. 83 (2011) 6474–6484.
[6] A.S. Whale, J.F. Huggett, S. Cowen, V. Speirs, J. Shaw, S. Ellison, C.A. Foy, D.J. Scott, Comparison of microfluidic digital PCR and conventional quantitative PCR for measuring copy number variation, Nucleic Acids Res. 40 (2012) e82.
[7] R. Sanders, D.J. Mason, C.A. Foy, J.F. Huggett, Evaluation of digital PCR for absolute RNA quantification, PLoS One 8 (2013) e75296.
[8] C.M. Hindson, J.R. Chevillet, H.A. Briggs, E.N. Gallichotte, I.K. Ruf, B.J. Hindson, R.L. Vessella, M. Tewari, Absolute quantification by droplet digital PCR versus analog real-time PCR, Nat. Methods 10 (2013) 1003–1005.
[9] J.F. Huggett, J. Garson, A.S. Whale, Digital PCR and its potential application to microbiology, in: D.H. Persing, F.C. Tenover, Y. Tang, F.S. Nolte, R.T. Hayden, A. van Belkum (Eds.), Molecular Microbiology: Diagnostic Principles and Practice, 3rd ed., ASM Press Washington DC, 2016, pp. 49–57.
[10] M.J. Burns, A.M. Burrell, C.A. Foy, The applicability of digital PCR for the assessment of detection limits in GMO analysis, Eur. Food Res. Technol. 231 (2010) 353–362.
[11] D. Morisset, D. Štebih, M. Milavec, K. Gruden, J. Žel, Quantitative analysis of food and feed samples with droplet digital PCR, PLoS One 8 (2013) e62583.
[12] R. Nitcher, A. Distelfeld, C. Tan, L. Yan, J. Dubcovsky, Increased copy number at the HvFT1 locus is associated with accelerated flowering time in barley, Mol. Genet. Genom. 288 (2013) 261–275.
[13] A. Zmienko, A. Samelak, P. Kozlowski, M. Figlerowicz, Copy number polymorphism in plant genomes, Theor. Appl. Genet. 127 (2014) 1–18.
[14] L. Warren, D. Bryder, I.L. Weissman, S.R. Quake, Transcription factor profiling in individual hematopoietic progenitors by digital RT-PCR, Proc. Natl. Acad. Sci. 103 (2006) 17807–178012.
[15] J.L. Ku, Y.K. Jeon, J.G. Park, Methylation-specific PCR, Methods Mol. Biol. (Clifton, N.J.) 791 (2011) 23–32.
[16] P.S. Mitchell, R.K. Parkin, E.M. Kroh, B.R. Fritz, S.K. Wyman, E.L. Pogosova-Agadjanyan, A. Peterson, J. Noteboom, K.C. O'Briant, A. Allen, Circulating microRNAs as stable blood-based markers for cancer detection, Proc. Natl. Acad. Sci. U. S. A. 105 (2008) 10513–10518.
[17] B.J. Hindson, K.D. Ness, D.A. Masquelier, P. Belgrader, N.J. Heredia, A.J. Makarewicz, I.J. Bright, M.Y. Lucero, A.L. Hiddessen, T.C. Legler, et al., High-throughput droplet digital PCR system for absolute quantitation of DNA copy number, Anal. Chem. 83 (2011) 8604–8610.
[18] H.C. Fan, S.R. Quake, Detection of aneuploidy with digital polymerase chain reaction, Anal. Chem. 79 (2007) 7576–7579.
[19] J.F. Huggett, S. Cowen, C.A. Foy, Considerations for digital PCR as an accurate molecular diagnostic tool, Clin. Chem. 61 (2015) 79–88.
[20] V. Taly, D. Pekin, L. Benhaim, S.K. Kotsopoulos, D. Le Corre, X. Li, I. Atochin, D.R. Link, A.D. Griffiths, K. Pallier, et al., Multiplex picodroplet digital PCR to detect KRAS mutations in circulating DNA from the plasma of colorectal cancer patients, Clin. Chem. 59 (2013) 1722–1731.
[21] P. Laurent-Puig, D. Pekin, C. Normand, S.K. Kotsopoulos, P. Nizard, K. Perez-Toralla, R. Rowell, J. Olson, P. Srinivasan, D. Le Corre, Clinical relevance of KRAS-mutated subclones detected with picodroplet digital PCR in advanced colorectal cancer treated with anti-EGFR therapy, Clin. Cancer Res. 21 (2015) 1087–1097.
[22] S. Pholwat, S. Stroup, S. Foongladda, E. Houpt, Digital PCR to detect and quantify heteroresistance in drug resistant *Mycobacterium tuberculosis*, PLoS One 8 (2013) e57238.
[23] A.S. Whale, C. Bushell, P.R. Grant, S. Cowen, I. Guttierrez-Aguirre, D.M. O'Sullivan, J. Zel, M. Milavec, C.A. Foy, E. Nastouli, et al., Detection of rare drug resistance mutations by digital PCR in a human influenza A virus model system and clinical samples, J. Clin. Microbiol. 54 (2016) 392–400.
[24] N. Lench, A. Barrett, S. Fielding, F. McKay, M. Hill, L. Jenkins, H. White, L.S. Chitty, The clinical implementation of non-invasive prenatal diagnosis for single-gene disorders: challenges and progress made, Prenat. Diagn. 33 (2013) 555–562.
[25] A.N. Barrett, T.C.R. McDonnell, K.C.A. Chan, L.S. Chitty, Digital PCR analysis of maternal plasma for noninvasive detection of sickle cell anemia, Clin. Chem. 58 (2012) 1026–1032.
[26] J. Beck, S. Bierau, S. Balzer, R. Andag, P. Kanzow, J. Schmitz, J. Gaedcke, O. Moerer, J.E. Slotta, P. Walson, Digital droplet PCR for rapid quantification of donor DNA in the circulation of transplant recipients as a potential universal biomarker of graft injury, Clin. Chem. 59 (2013) 1732–1741.
[27] G.R. Oxnard, C.P. Paweletz, Y. Kuang, S.L. Mach, A. O'Connell, M.M. Messineo, J.J. Luke, M. Butaney, P. Kirschmeier, D.M. Jackman, et al., Noninvasive detection of response and resistance in EGFR-mutant lung cancer using quantitative next-generation genotyping of cell-free plasma DNA, Clin. Cancer Res. 20 (2014) 1698–1705.
[28] I. Garcia-Murillas, G. Schiavon, B. Weigelt, C. Ng, S. Hrebien, R.J. Cutts, M. Cheang, P. Osin, A. Nerurkar, I. Kozarewa, Mutation tracking in circulating tumor DNA predicts relapse in early breast cancer, Sci. Transl. Med. 7 (2015) 302ra133.
[29] G. Siravegna, A. Bardelli, Minimal residual disease in breast cancer: in blood veritas, Clin. Cancer Res. 20 (2014) 2505–2507.
[30] E. Navarro, G. Serrano-Heras, M.J. Castano, J. Solera, Real-time PCR detection chemistry, Clin. Chim. Acta 439 (2015) 231–250.
[31] S. Dube, J. Qin, R. Ramakrishnan, Mathematical analysis of copy number variation in a DNA sample using digital PCR on a nanofluidic device, PLoS One 3 (2008) e2876.
[32] S. Bhat, N. Curach, T. Mostyn, G.S. Bains, K.R. Griffiths, K.R. Emslie, Comparison of methods for accurate quantification of DNA mass concentration with traceability to the international system of units, Anal. Chem. 82 (2010) 7185–7192.
[33] S. Bhat, J.L. McLaughlin, K.R. Emslie, Effect of sustained elevated temperature prior to amplification on template copy number estimation using digital polymerase chain reaction, Analyst 136 (2011) 724–732.
[34] A.S. Whale, S. Cowen, C.A. Foy, J.F. Huggett, Methods for applying accurate digital PCR analysis on low copy DNA samples, PLoS One 8 (2013) e58177.
[35] G.P. McDermott, D. Do, C.M. Litterst, D. Maar, C.M. Hindson, E.R. Steenblock, T.C. Legler, Y. Jouvenot, S.H. Marrs, A. Bemis, et al., Multiplexed target detection using DNA-binding dye chemistry in droplet digital PCR, Anal. Chem. 85 (2013) 11619–11627.
[36] D. Sint, L. Raso, M. Traugott, Advances in multiplex PCR: balancing primer efficiencies and improving detection success, Methods Ecol. Evol. 3 (2012) 898–905.
[37] N.J. Heredia, P. Belgrader, S. Wang, R. Koehler, J. Regan, A.M. Cosman, S. Saxonov, B. Hindson, S.C. Tanner, A.S. Brown, Droplet digital PCR quantitation of HER2 expression in FFPE breast cancer samples, Methods 59 (2013) S20–23.
[38] P. Belgrader, S.C. Tanner, J.F. Regan, R. Koehler, B.J. Hindson, A.S. Brown, Droplet digital PCR measurement of HER2 copy number alteration in formalin-fixed paraffin-embedded breast carcinoma tissue, Clin. Chem. 59 (2013) 991–994.
[39] H. Gevensleben, I. Garcia-Murillas, M.K. Graeser, G. Schiavon, P. Osin, M. Parton, I.E. Smith, A. Ashworth, N.C. Turner, Noninvasive detection of HER2 amplification with plasma DNA digital PCR, Clin. Cancer Res. 19 (2013) 3276–3284.
[40] G. Zhu, X. Ye, Z. Dong, Y.C. Lu, Y. Sun, Y. Liu, R. McCormack, Y. Gu, X. Liu, Highly sensitive droplet digital PCR method for detection of EGFR-activating mutations in plasma cell-free DNA from patients with advanced non-small cell lung cancer, J. Mol. Diagn. 17 (2015) 265–272.
[41] M.F. Sanmamed, S. Fernandez-Landazuri, C. Rodriguez, R. Zarate, M.D. Lozano, L. Zubiri, J.L. Perez-Gracia, S. Martin-Algarra, A. Gonzalez, Quantitative cell-free circulating BRAFV600E mutation analysis by use of droplet digital PCR in the follow-up of patients with melanoma being treated with BRAF inhibitors, Clin. Chem. 61 (2015) 297–304.
[42] A.L. Reid, J.B. Freeman, M. Millward, M. Ziman, E.S. Gray, Detection of BRAF-V600E and V600K in melanoma circulating tumour cells by droplet digital PCR, Clin. Biochem. 48 (2015) 999–1002.

[43] K.A. Heyries, C. Tropini, M. Vaninsberghe, C. Doolin, O.I. Petriv, A. Singhal, K. Leung, C.B. Hughesman, C.L. Hansen, Megapixel digital PCR, Nat. Methods 8 (2011) 649–651.
[44] L.B. Pinheiro, V.A. Coleman, C.M. Hindson, J. Herrmann, B.J. Hindson, S. Bhat, K.R. Emslie, Evaluation of a droplet digital polymerase chain reaction format for DNA copy number quantification, Anal. Chem. 84 (2012) 1003–1011.
[45] L. Miotke, B.T. Lau, R.T. Rumma, H.P. Ji, High sensitivity detection and quantitation of DNA copy number and single nucleotide variants with single color droplet digital PCR, Anal. Chem. 86 (2014) 2618–2624.
[46] Q. Zhong, S. Bhattacharya, S. Kotsopoulos, J. Olson, V. Taly, A.D. Griffiths, D.R. Link, J.W. Larson, Multiplex digital PCR: breaking the one target per color barrier of quantitative PCR, Lab Chip 11 (2011) 2167–2174.
[47] A. Didelot, S.K. Kotsopoulos, A. Lupo, D. Pekin, X. Li, I. Atochin, P. Srinivasan, Q. Zhong, J. Olson, D.R. Link, et al., Multiplex picoliter-droplet digital PCR for quantitative assessment of DNA integrity in clinical samples, Clin. Chem. 59 (2013) 815–823.
[48] J.F. Regan, N. Kamitaki, T. Legler, S. Cooper, N. Klitgord, G. Karlin-Neumann, C. Wong, S. Hodges, R. Koehler, S. Tzonev, et al., A rapid molecular approach for chromosomal phasing, PLoS One 10 (2015) e0118270.
[49] H.L. Lund, C.B. Hughesman, K. McNeil, S. Clemens, K. Hocken, R. Pettersson, A. Karsan, L.J. Foster, C. Haynes, Initial diagnosis of chronic myelogenous leukemia based on quantification of M-BCR status using droplet digital PCR, Anal. Bioanal. Chem. 408 (2016) 1079–1094.
[50] A.S. Devonshire, I. Honeyborne, A. Gutteridge, A.S. Whale, G. Nixon, P. Wilson, G. Jones, T.D. McHugh, C.A. Foy, J.F. Huggett, Highly reproducible absolute quantification of Mycobacterium tuberculosis complex by digital PCR, Anal. Chem. 87 (2015) 3706–3713.
[51] G. Nixon, J.A. Garson, P. Grant, E. Nastouli, C.A. Foy, J.F. Huggett, A comparative study of sensitivity, linearity and resistance to inhibition of digital and non-digital PCR and LAMP assays for quantification of human cytomegalovirus, Anal. Chem. 86 (2014) 4387–4394.
[52] M. Jones, J. Williams, K. Gärtner, R. Phillips, J. Hurst, J. Frater, Low copy target detection by droplet digital PCR through application of a novel open access bioinformatic pipeline, 'definetherain', J. Virol. Methods 202 (2014) 46–53.
[53] T. Dreo, M. Pirc, Z. Ramsak, J. Pavsic, M. Milavec, J. Zel, K. Gruden, Optimising droplet digital PCR analysis approaches for detection and quantification of bacteria: a case study of fire blight and potato brown rot, Anal. Bioanal. Chem. 406 (2014) 6513–6528.
[54] A. Lievens, S. Jacchia, D. Kagkli, C. Savini, M. Querci, Measuring digital PCR quality: performance parameters and their optimization, PLoS One 11 (2016) e0153317.